JOINT ANGLE AND FREQUENCY ESTIMATION USING STRUCTURED LEAST SQUARES

Cheng Qian[1]*, Lei Huang*[1]*, Yunmei Shi*[1] *and H. C. So*[2]

[1]Department of Electronic and Information Engineering
Harbin Institute of Technology Shenzhen Graduate School, Shenzhen, China
[2]Department of Electronic Engineering
City University of Hong Kong, Hong Kong, China

ABSTRACT

A structured least squares based ESPRIT method is devised for joint direction-of-arrival and frequency estimation. By considering the errors in the estimated signal subspace and employing an iterative minimization procedure, the proposed approach is able to efficiently refine the estimated signal subspace, leading to significant enhancement in estimation performance. Simulation results demonstrate the effectiveness of the proposed approach.

1. INTRODUCTION

In spatial-temporal radio channel measurement, it is of considerable interest to jointly estimating the direction-of-arrival (DOA) and frequencies of known signals. It has several applications, such as radar, sonar and mobile communication. A precise estimation of DOAs and frequencies of signals of interest can help to provide better channel information in support of improved link quality.

Numerous methods have been developed for joint DOA and frequency estimation. The maximum likelihood (ML) estimate [1] is theoretically optimal and it is equivalent to the least squares estimate under white Gaussian noise situation. Although the ML estimate has excellent statistical properties, it requires a multidimensional optimization which is computationally intensive. ESPRIT-like algorithms [3]-[4] have been proposed to balance the estimation accuracy and computational complexity. Lemma *et al.* [3] has introduced the ESPRIT algorithm for joint DOA and frequency estimation. However, when the signals have approximately the same frequencies, its performance will decrease severely. In [4], the authors have presented a joint angle and frequency estimation (JAFE) algorithm that utilizes the temporal-spatial smoothing technique to preprocess the sample data, and then uses the ESPRIT algorithm to estimate the DOA and frequency parameters. However, the optimal temporal factor m_o is hard to obtain in many applications since m_o is a linear function of the sample size N, i.e., $m_o \approx (3N+2)/5$. Moreover, as the sample size becomes larger, its computational complexity will increase by $O(m_o^3)$.

In this paper, we propose a structured least squares (SLS) based ESPRIT approach for joint DOA and frequency estimation. Unlike the conventional ESPRIT algorithm [3]-[4], our proposal employs the forward-backward averaging covariance matrix to replace the sample covariance matrix. In addition, a SLS method is utilized to solve the rotational invariance equations to obtain robust DOA and frequency estimates. Numerical results demonstrates that the developed scheme is superior to the ESPRIT and JAFE methods.

2. PROBLEM FORMULATION

Consider a uniform linear array (ULA) with M omnidirectional antennas. Let f_c be the center frequency of the band of the interest. Assume that there are P $(P < M)$ narrow-band source signals $\{d_p(t)\}$, with center frequencies $f_c + f_p$, $p = 1, \cdots, P$, imping on the array from directions $\{\theta_1, \cdots, \theta_P\}$ in the far field. After down-conversion to baseband, the $M \times 1$ observation vector is

$$\begin{aligned}\mathbf{x}(t) &= \sum_{i=1}^{P} \mathbf{a}(\theta_i) d_i(t) e^{j2\pi f_i t/F} + \mathbf{n}(t) \\ &= \mathbf{A}\mathbf{\Phi}^t \mathbf{d}(t) + \mathbf{n}(t) \end{aligned} \quad (1)$$

where F is the sample rate, $\mathbf{d}(t) = [d_1(t), \cdots, d_P(t)]^T$ is the source signal vector with $(\cdot)^T$ being the transpose, $\mathbf{n}(t)$ is the additive white Gaussian process with zero mean and variance $\sigma_n^2 \mathbf{I}_M$, $\mathbf{I}_M$ is a $M \times M$ identity matrix, and $\mathbf{A} = [\mathbf{a}(\theta_1), \cdots, \mathbf{a}(\theta_P)]$ is the array manifold with

$$\mathbf{a}(\theta_p) = \left[1, e^{-j2\pi \sin\theta_p d/\lambda}, \cdots, e^{-j2\pi(M-1)\sin\theta_p d/\lambda}\right]^T \quad (2)$$

being the pth steering vector, and

$$\mathbf{\Phi} = \text{diag}\{e^{j2\pi f_1/F}, \cdots, e^{j2\pi f_P/F}\}. \quad (3)$$

The work described in this paper was in part supported by a grant from the NSFC/RGC Joint Research Scheme sponsored by the Research Grants Council of Hong Kong and the National Natural Science Foundation of China (Project No.: N_CityU 104/11, 61110229/61161160564), by the National Natural Science under Grants 61222106 and 61171187 and by the Shenzhen Kongqie talent program under Grant KQC201109020061A.

Here, λ is the carrier wavelength and $d = \lambda/2$ is the interelement spacing.

3. PROPOSED ALGORITHM

3.1. Data Processing

We assume that the narrowband signals are block fading that $\{d_p(k)\}$ remain unchanged in a short sampling interval, i.e.,

$$\mathbf{d}(t) \approx \mathbf{d}\left(t + \frac{1}{F}\right) \approx \cdots \approx \mathbf{d}\left(t + \frac{m-1}{F}\right). \quad (4)$$

This means that, for the same sampling period, the first m ($m \ll F$) samples are approximately the same. It allows us to collect m sample subsets with each subset containing N samples. As a result, similar to [3], the data matrix is formed as

$$\mathbf{X} = \begin{bmatrix} \mathbf{x}(0) & \mathbf{x}(1) & \cdots & \mathbf{x}(N-1) \\ \mathbf{x}\left(\frac{1}{F}\right) & \mathbf{x}\left(1+\frac{1}{F}\right) & \cdots & \mathbf{x}\left(N-1+\frac{1}{F}\right) \\ \vdots & \vdots & \ddots & \vdots \\ \mathbf{x}\left(\frac{m-1}{F}\right) & \mathbf{x}\left(1+\frac{m-1}{F}\right) & \cdots & \mathbf{x}\left(N-1+\frac{m-1}{F}\right) \end{bmatrix}. \quad (5)$$

Substituting (1) and (4) into (5) yields

$$\mathbf{X} \approx \mathbf{A}_m \mathbf{D}_m + \mathbf{N}_m \quad (6)$$

where

$$\mathbf{A}_m = \left[(\mathbf{A})^T \quad (\mathbf{A}\mathbf{\Phi})^T \quad \cdots \quad (\mathbf{A}\mathbf{\Phi}^{m-1})^T\right]^T \quad (7)$$

$$\mathbf{D}_m = \left[\mathbf{d}(0) \quad \mathbf{\Phi}\mathbf{d}\left(\tfrac{1}{F}\right) \quad \cdots \quad \mathbf{\Phi}^{N-1}\mathbf{d}\left(\tfrac{N-1}{F}\right)\right] \quad (8)$$

$$\mathbf{N}_m = \left[\mathbf{n}(0) \quad \mathbf{n}\left(\tfrac{1}{F}\right) \quad \cdots \quad \mathbf{n}\left(\tfrac{N-1}{F}\right)\right]. \quad (9)$$

Let

$$\tilde{\mathbf{\Phi}} = \begin{bmatrix} 1 & \cdots & 1 \\ e^{j2\pi f_1/F} & \cdots & e^{j2\pi f_P/F} \\ \vdots & \ddots & \vdots \\ e^{j2\pi f_1(m-1)/F} & \cdots & e^{j2\pi f_P(m-1)/F} \end{bmatrix}. \quad (10)$$

Then (6) can be rewritten as

$$\mathbf{X} \approx (\tilde{\mathbf{\Phi}} \odot \mathbf{A})\mathbf{D}_m + \mathbf{N}_m \quad (11)$$

where $\odot$ is the Khatri-Rao product.

3.2. Joint DOA and Frequency Estimation

Let $\hat{\mathbf{R}} = \mathbf{X}_m\mathbf{X}_m^H/N \in \mathbb{C}^{mM\times mM}$ be the sample covariance matrix of $\mathbf{X}_m$. When the source signals are correlated, $\hat{\mathbf{R}}$ will be poorly estimated. Therefore, we use the forward-backward averaging matrix [7] to replace $\hat{\mathbf{R}}$, i.e.,

$$\mathbf{R} = \frac{1}{2}\left(\hat{\mathbf{R}} + \mathbf{\Pi}\hat{\mathbf{R}}^*\mathbf{\Pi}\right) \quad (12)$$

where $\mathbf{\Pi}$ is the exchange matrix with one on its antidiagonal and zeros elsewhere, and $(\cdot)^*$ stands for complex conjugate. Note that the P eigenvectors corresponding to the P largest eigenvalues are used to form the signal subspace $\mathbf{U}_s$, that is, span$\{\mathbf{U}_s\}$ = span$\{\mathbf{A}_m\}$.

We begin the estimation of DOA and spatial frequency by defining the following two select matrices:

$$\begin{cases} \mathbf{J}_\theta^{\uparrow} = \mathbf{I}_m \otimes [\mathbf{I}_{M-1} \quad \mathbf{0}_1] & (13a) \\ \mathbf{J}_\theta^{\downarrow} = \mathbf{I}_m \otimes [\mathbf{0}_1 \quad \mathbf{I}_{M-1}] & (13b) \end{cases}$$

and

$$\begin{cases} \mathbf{J}_f^{\uparrow} = [\mathbf{I}_{m-1} \quad \mathbf{0}_1] \otimes \mathbf{I}_M & (14a) \\ \mathbf{J}_f^{\downarrow} = [\mathbf{0}_1 \quad \mathbf{I}_{m-1}] \otimes \mathbf{I}_M. & (14b) \end{cases}$$

where $\otimes$ is the kronecker product and $\mathbf{0}_1$ is a $(M-1)\times 1$ zero vector. Then the rotational invariance equations for DOA and frequency estimation can be expressed as

$$\mathbf{J}_\theta^{\uparrow}\mathbf{U}_s\mathbf{\Psi}_\theta = \mathbf{J}_\theta^{\downarrow}\mathbf{U}_s \quad (15a)$$

$$\mathbf{J}_f^{\uparrow}\mathbf{U}_s\mathbf{\Psi}_f = \mathbf{J}_f^{\downarrow}\mathbf{U}_s \quad (15b)$$

where

$$\mathbf{\Psi}_\theta = \mathbf{T}\mathbf{\Theta}\mathbf{T}^{-1} \quad (16a)$$

$$\mathbf{\Psi}_f = \mathbf{T}\mathbf{\Phi}\mathbf{T}^{-1} \quad (16b)$$

with $\mathbf{T}$ being a $P \times P$ nonsingular matrix and

$$\mathbf{\Theta} = \text{diag}\{e^{j2\pi \sin\theta_1 d/\lambda}, \cdots, e^{j2\pi \sin\theta_P d/\lambda}\}. \quad (17)$$

By solving (15) and performing the eigenvalue decomposition of $\mathbf{\Theta}$ and $\mathbf{\Phi}$, we obtain the DOA and frequency estimates as

$$\hat{\theta}_i = \sin^{-1}\left(\frac{\lambda \cdot \angle(\alpha_i)}{2\pi d}\right) \quad (18)$$

$$\hat{f}_i = \frac{F \cdot \angle(\beta_i)}{2\pi}, \quad i = 1, \cdots, P \quad (19)$$

where $\angle$ represents the angle operator, α_i and β_i are the ith eigenvalues of $\mathbf{\Psi}_\theta$ and $\mathbf{\Psi}_f$, respectively.

In [3] and [4], the authors utilize the least squares (L-S) to solve (15). However, (15) is a highly structured and overdetermined equation. With the increase of the overlapping elements in (15), the performance of the LS solutions will decrease, as has been pointed out in [10]. This is due to the fact that, in the LS method, it is assumed that $\mathbf{J}_\theta^{\uparrow}\mathbf{U}_s$ and $\mathbf{J}_f^{\uparrow}\mathbf{U}_s$ are known without error, and only the errors in $\mathbf{J}_\theta^{\downarrow}\mathbf{U}_s$ and $\mathbf{J}_f^{\downarrow}\mathbf{U}_s$ are minimized. However, such an assumption is not valid in our problem. In fact, each term in (15) has errors. Therefore, we assume that there exists errors in $\mathbf{U}_s$, $\mathbf{\Psi}_\theta$ and $\mathbf{\Psi}_f$. Hence, their improved estimates can be formulated as $\bar{\mathbf{U}}_s = \mathbf{U}_s + \Delta\mathbf{U}_s$, $\bar{\mathbf{\Psi}}_\theta = \mathbf{\Psi}_\theta + \Delta\mathbf{\Psi}_\theta$ and $\bar{\mathbf{\Psi}}_f = \mathbf{\Psi}_f + \Delta\mathbf{\Psi}_f$.

In order to minimize $\Delta\mathbf{U}_s$, $\Delta\mathbf{\Psi}_\theta$ and $\Delta\mathbf{\Psi}_f$, we need to use an iterative minimization procedure.

Meanwhile, let us define two residual matrices

$$\mathbf{E}_\theta = \mathbf{J}_\theta^{\uparrow}\bar{\mathbf{U}}_s\bar{\mathbf{\Psi}}_\theta - \mathbf{J}_\theta^{\downarrow}\bar{\mathbf{U}}_s \tag{20a}$$

$$\mathbf{E}_f = \mathbf{J}_f^{\uparrow}\bar{\mathbf{U}}_s\bar{\mathbf{\Psi}}_f - \mathbf{J}_f^{\uparrow}\bar{\mathbf{U}}_s. \tag{20b}$$

At the kth iteration, let $\bar{\mathbf{U}}_{s,k} = \mathbf{U}_{s,k-1} + \Delta\mathbf{U}_{s,k-1}$, $\bar{\mathbf{\Psi}}_{\theta,k} = \mathbf{\Psi}_{\theta,k-1} + \Delta\mathbf{\Psi}_{\theta,k-1}$ and $\bar{\mathbf{\Psi}}_{f,k} = \mathbf{\Psi}_{f,k-1} + \Delta\mathbf{\Psi}_{f,k-1}$ be the refined matrices of $\bar{\mathbf{U}}$, $\bar{\mathbf{\Psi}}_\theta$ and $\bar{\mathbf{\Psi}}_f$, respectively. Meanwhile, let $\mathbf{E}_{\theta,k}$ and $\mathbf{E}_{\theta,k}$ be the residual matrices. Therefore, at the $(k+1)$th iteration, by neglecting the second-order term $\Delta\mathbf{U}_{s,k}\Delta\mathbf{\Psi}_{\theta,k}$ and $\Delta\mathbf{U}_{s,k}\Delta\mathbf{\Psi}_{f,k}$, we obtain

$$\begin{aligned}\mathbf{E}_{\theta,k+1} \approx{}& \mathbf{E}_{\theta,k} + \mathbf{J}_\theta^{\uparrow}\mathbf{U}_{s,k}\Delta\mathbf{\Psi}_{\theta,k} + \mathbf{J}_\theta^{\uparrow}\Delta\mathbf{U}_{s,k}\mathbf{\Psi}_{\theta,k} \\ &- \mathbf{J}_\theta^{\downarrow}\Delta\mathbf{U}_{s,k}\end{aligned} \tag{21a}$$

$$\begin{aligned}\mathbf{E}_{f,k+1} \approx{}& \mathbf{E}_{f,k} + \mathbf{J}_f^{\uparrow}\mathbf{U}_{s,k}\Delta\mathbf{\Psi}_{f,k} + \mathbf{J}_f^{\uparrow}\Delta\mathbf{U}_{s,k}\mathbf{\Psi}_{f,k} \\ &- \mathbf{J}_f^{\downarrow}\Delta\mathbf{U}_{s,k}.\end{aligned} \tag{21b}$$

It follows from (21) that

$$\begin{aligned}&\mathrm{vec}\left\{\mathbf{E}_{\theta,k+1}\right\} \approx \mathrm{vec}\left\{\mathbf{E}_{\theta,k}\right\} + \left[\mathbf{I}_P \otimes (\mathbf{J}_\theta^{\uparrow}\mathbf{U}_{s,k})\right] \times \\ &\mathrm{vec}\left\{\Delta\mathbf{\Psi}_{\theta,k}\right\} + \left[\mathbf{\Psi}_{\theta,k}^T \otimes \mathbf{J}_\theta^{\uparrow} - \mathbf{I}_P \otimes \mathbf{J}_\theta^{\downarrow}\right] \times \mathrm{vec}\left\{\Delta\mathbf{U}_{s,k}\right\}\end{aligned} \tag{22a}$$

$$\begin{aligned}&\mathrm{vec}\left\{\mathbf{E}_{f,k+1}\right\} \approx \mathrm{vec}\left\{\mathbf{E}_{f,k}\right\} + \left[\mathbf{I}_P \otimes (\mathbf{J}_f^{\uparrow}\mathbf{U}_{s,k})\right] \times \\ &\mathrm{vec}\left\{\Delta\mathbf{\Psi}_{f,k}\right\} + \left[\mathbf{\Psi}_{f,k}^T \otimes \mathbf{J}_f^{\uparrow} - \mathbf{I}_P \otimes \mathbf{J}_f^{\downarrow}\right] \times \mathrm{vec}\left\{\Delta\mathbf{U}_{s,k}\right\}\end{aligned} \tag{22b}$$

where vec$\{\cdot\}$ is the vectorization operator. In addition, we define $\Delta\mathbf{U}_k = \sum_{i=1}^{k-1}\Delta\mathbf{U}_{s,i}$ as the signal subspace estimation error matrix at the kth iteration. Arrange (22) into matrix form yields the following SLS problem

$$\min_{\Delta\mathbf{\Psi}_{\theta,k},\Delta\mathbf{\Psi}_{f,k}} \left|\left|\mathbf{H}_k \cdot \begin{bmatrix}\mathrm{vec}\left\{\Delta\mathbf{\Psi}_{\theta,k}\right\} \\ \mathrm{vec}\left\{\Delta\mathbf{\Psi}_{f,k}\right\} \\ \mathrm{vec}\left\{\Delta\mathbf{U}_{s,k}\right\}\end{bmatrix} + \begin{bmatrix}\mathrm{vec}\left\{\mathbf{E}_{\theta,k}\right\} \\ \mathrm{vec}\left\{\mathbf{E}_{f,k}\right\} \\ \kappa \cdot \mathrm{vec}\{\Delta\mathbf{U}_k\}\end{bmatrix}\right|\right|^2 \tag{23}$$

where $\kappa > 1$ is a user defined parameter [1] that keeps the entries of $\Delta\mathbf{U}_s$ be larger than those of $\mathbf{E}_\theta$ and $\mathbf{E}_f$, and

$$\mathbf{H}_k = \begin{bmatrix}\mathbf{I}_P \otimes (\mathbf{J}_\theta^{\uparrow}\mathbf{U}_{s,k}) & \mathbf{0} & \mathbf{\Psi}_{\theta,k}^T \otimes \mathbf{J}_\theta^{\uparrow} - \mathbf{I}_P \otimes \mathbf{J}_\theta^{\downarrow} \\ \mathbf{0} & \mathbf{I}_P \otimes (\mathbf{J}_f^{\uparrow}\mathbf{U}_{s,k}) & \mathbf{\Psi}_{f,k}^T \otimes \mathbf{J}_f^{\uparrow} - \mathbf{I}_P \otimes \mathbf{J}_f^{\downarrow} \\ \mathbf{0} & \mathbf{0} & \kappa\mathbf{I}_{mMP}\end{bmatrix}.$$

[1] There is no definite way to determine κ. But similar to [10], we can alternatively choose $\kappa = \sqrt{(m(M-1)+M(m-1))/\alpha mM}$ where α is also a user defined factor. Actually, the performance of our solution is not sensitive to the chosen of κ. The presented simulation results were obtained for $\kappa = 5$, whe1reas $\kappa = 30$ and $\kappa = 100$ produced almost the same performance.

In our study, we use the LS solutions, $\mathbf{\Psi}_\theta^{\mathrm{LS}}$, $\mathbf{\Psi}_f^{\mathrm{LS}}$ and $\mathbf{U}_s^{\mathrm{LS}}$ as the initialized estimates of $\mathbf{\Phi}_\theta$, $\mathbf{\Phi}_f$ and $\mathbf{E}_s$. The iteration stopping condition is

$$\min\{||\Delta\mathbf{\Psi}_{\theta,k}||_F^2, ||\Delta\mathbf{\Psi}_{f,k}||_F^2, ||\Delta\mathbf{U}_{s,k}||_F^2\} \le \epsilon \tag{24}$$

where ϵ is predefined small positive constant. When the algorithm converges at the kth iteration, we use $\mathbf{\Psi}_\theta^{\mathrm{SLS}} = \mathbf{\Psi}_{\theta,k} + \Delta\mathbf{\Psi}_{\theta,k}$ and $\mathbf{\Psi}_f^{\mathrm{SLS}} = \mathbf{\Psi}_{f,k} + \Delta\mathbf{\Psi}_{f,k}$ as the final estimates of $\mathbf{\Psi}_\theta$ and $\mathbf{\Psi}_f$, respectively. The DOA and frequency estimates are eventually computed from (18)-(19).

3.3. Computational Complexity

We first analyze the complexity of the JADE algorithm. It is clear that the computing of the sample covariance and its EVD account for most of the complexity of the JADE method. The complexity of computing $\mathbf{R}$ in (12) is $\mathcal{O}(m^2M^2N)$ and the EVD of $\mathbf{R}$ is $\mathcal{O}(m^3M^3)$. Hance, the complexity for JADE is about $\mathcal{O}(m^2M^2N + m^3M^3)$. For the proposed scheme, the additional computational burden is caused by the iteration procedure utilized to solve (23). In each iteration step, a least squares solver is employed to obtain $\Delta\mathbf{\Phi}_{\theta,k}$, $\Delta\mathbf{\Phi}_{f,k}$ and $\Delta\mathbf{E}_{s,k}$. The complexity for this procedure is about $\mathcal{O}(10m^3M^3P^3)$ since $\mathbf{H}_k$ is a $(3MNP - mP - MP) \times (2P^2 + mMP)$ matrix and we have $mM > P$, $mM > m$ and $mM > M$. Therefore, for the proposed method, the computational complexity is about $\mathcal{O}(10Km^3M^3P^3)$ where K is the number of iterations. Note that for the SLS, two iterations are enough to provide a considerable accuracy.

4. SIMULATION

The performance of the proposed algorithm is compared to the ESPRIT [3] and JAFE [4] algorithms in terms of root mean square error (RMSE). We consider a ULA of $M = 7$ sensors successively separated by a half-wavelength. The noise is white Gaussian process with zeros mean and unit variance. For the JAFE algorithm, as suggested in [4], L is selected as $L \approx 0.4M$. In the sequel, we set $L = 3$. Furthermore, we set $m = 3$ in (6). The number of snapshots is $N = 64$. The tolerance parameter of the proposed algorithm is set to be $\epsilon = 10^{-7}$. We also assume the number of signals is known or estimated by [11] All the results are based on 1000 independent trials.

Example 1: In this example, we examine the RMSE performance as a function of signal-to-noise ratio (SNR). We set $\sigma_n^2 = 1$ and vary the signal power such that the input SNR goes from -6dB to 30dB. Three equal-power narrowband signals are assumed to imping upon the array from directions $\theta_1 = 10°$, $\theta_2 = 19°$ and $\theta_3 = 30°$. The center frequencies of the signals are $f_1 = 2$MHz, $f_2 = 2.06$MHz and $f_3 = 2.2$MHz, respectively. For the JAFE algorithm [4], the temporal and spatial smoothing factors are both chosen to be

3. It is observed from Fig. 1 that the proposed method outperforms the ESPRIT and the JAFE algorithms for all the SNRs.

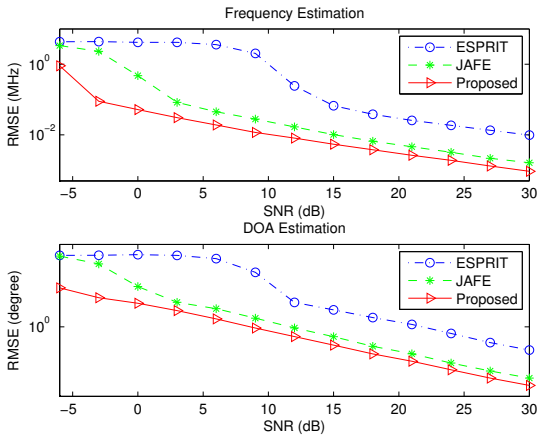

Fig. 1. RMSE versus SNR

Example 2: The experiment is devised to compare the DOA and frequency estimation errors as a function of the angular separation. The SNR is set as SNR= 0dB. We consider two signals in this example. The frequencies of the two signals are set to be $f_1 = 2$MHz and $f_2 = 2.15$MHz, and the DOA of the first signal is fixed at $\theta_1 = 0°$. We set the DOA of the second signal as $\theta_2 = 0° + \Delta\theta$ where $\Delta\theta$ is varied from $0°$ to $16°$. From Fig. 2, we can see that when angular separation is smaller than $6°$, the proposed algorithm outperforms its counterparts in both DOA and frequency estimation.

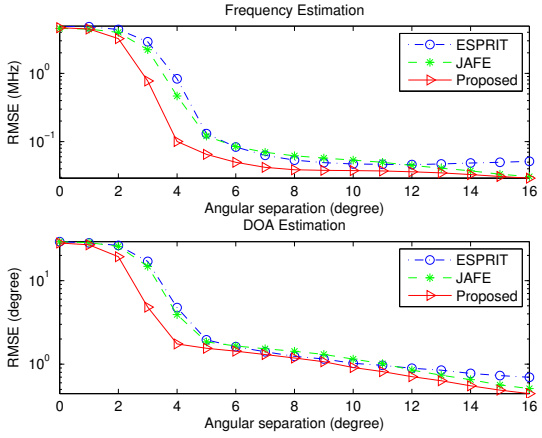

Fig. 2. RMSE versus angular separation

Example 3: Fig. 3 shows the RMSE performance as a function of frequency separation. We set the DOAs of two signals as $\theta_1 = 0°$ and $\theta_2 = 6°$. The frequency of the first signal is $f_1 = 2$MHz. The frequency of the second signal is $f_2 = (2 + \Delta f)$MHz where Δ_f is varied from 0kHz to 200kHz. Note that in small frequency separation, e.g., $\Delta f < 100$kHz, the two signals are temporally correlated. Due to the forward-backward averaging technique and the SLS method, it is observed from Fig. 3 that the proposed scheme outperforms the other two algorithms. When Δf is sufficiently large, the JAFE is a little bit inferior to the ESPRIT method, and the proposed and ESPRIT algorithms merge together.

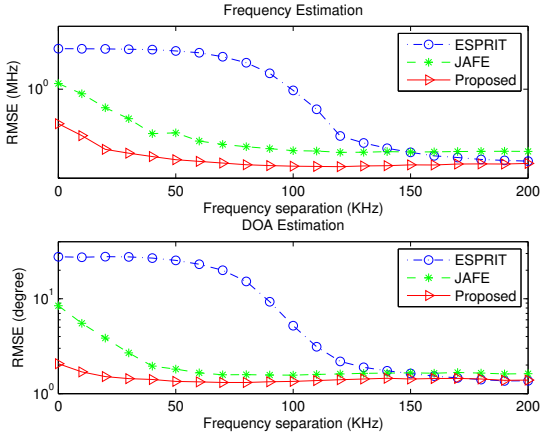

Fig. 3. RMSE versus frequency separation

5. CONCLUSION

A SLS-based ESPRIT algorithm for joint DOA and frequency estimation is devised in this paper. Unlike the existing ESPRIT, the proposed method considers the errors in the estimated signal subspace. Meanwhile, our proposal is able to utilize the SLS method to solve the rotational invariance equations, leading to significant enhancement in joint angle and frequency estimation performance. Computer simulation demonstrates the improvement of the proposed scheme.

6. REFERENCES

[1] M. A. Zatman and H. J. Strangeways, "An efficient joint direction of arrival and frequency ML estimator," in *Proc. IEEE Antennas Propagat. Symp.*, vol. 1, pp. 431-434, NewPort Beach, CA, USA, June, 1995.

[2] M. Wax and A. Leshem, "Joint estimation of time delays and directions of arrival of multiple reflections of a known signal," *IEEE Trans. Signal Process.*, vol. 45, no. 10, pp. 2477-2484, 1997.

[3] A. N. Lemma, A. van der Veen and E. F. Deprettere, "Joint angle-frequency estimation using multi-resolution," *Proc. IEEE Int. Conf., Acoustics, Speech, and Signal Processing*, vol. 4, pp. 1957-1960, Seattle, USA, 1998.

[4] A. N. Lemma, A. van der Veen and E. F. Deprettere, "Analysis of joint angle-frequency estimation using ESPRIT," *IEEE Trans. Signal Process.*, vol. 51, no. 5, pp. 1264-1283, 2003.

[5] A. van der Veen, M. Vanderveen and A. Paulraj, "Joint angle and delay estimation using shift-invariance techniques," *IEEE Trans. Signal Process.*, vol. 46, no. 5, pp. 405-418, 1998.

[6] M. Haardt and J. A. Nossek, "3-D unitary ESPRIT for joint 2-D angle and carrier estimation," *Proc. IEEE Int. Conf., Acoustics, Speech, and Signal Processing*, vol. 1, pp. 255-258, Munich, Bavaria, Germany, 1997.

[7] K. C. Huarng and C. C. Yeh, "A unitary transformation method for angle of arrival estimation," *IEEE Trans. Acoust., Speech, Signal Process.*, vol. 39, pp. 975-977, 1991.

[8] J. B. Rosen, H. Park and J. Glick, "Total least norm formulation and solution for structured problems," *SIAM J. Matrix Anal. Appl.*, vol. 17, no. 1, pp. 110-126, 1996.

[9] S. V. Huffel, H. Park and J. B. Rosen, "Formulation and solution of structured total least norm problems for parameter estimation," *IEEE Trans. Signal Process.*, vol. 44, no. 10, pp. 2464-2474, 1996.

[10] M. Haardt. "Structured least squares to improve the performance of ESPRIT-type algorithms," *IEEE Trans. Signal Process.*, vol. 45, no. 3, pp. 792-799, 1997.

[11] L. Huang and H. C. So, "Source Enumeration via MDL Criterion Based on Linear Shrinkage Estimation of Noise Subspace Covariance Matrix," *IEEE Transactions on Signal Processing,* vol. 61, no. 19, pp. 4806-4821, Oct. 2013.